

## §6. Impurity Behavior in V-4Cr-4Ti-Y Alloys Produced by Levitation Melting

Nagasaka, T., Muroga, T.,  
Hino, T., Satou, M., Abe, K., Chuto, T. (Tohoku Univ.),  
Ikubo, T. (Daido Bunseki Research, Inc.)

It has been clarified that reduction of oxygen level and control of Ti-C, N, O precipitate distribution are critical to improve workability, weldability and irradiation properties for V-4Cr-4Ti alloys. Yttrium (Y) addition is well known to be effective for reduction of oxygen level by oxide ( $Y_2O_3$ ) slug formation on the melting ingot surface. Because of the slug layer, the conventional large-scale melting processes, such as continuous arc-melting and electron beam melting, are not applicable to Y containing alloys. In the present paper, V-4Cr-4Ti-0.15Y alloy was fabricated by levitation melting.

Pure V, Cr and Ti used were the same grade as the reference high purity V-4Cr-4Ti alloy, NIFS-HEAT (NH). C, N and O impurity levels in Y were 210, 380 and 823 wppm, respectively. A 15 kg V-4Cr-4Ti-0.15Y ingot was melted under Ar gas ( $O_2$ : 0.62 ppm,  $N_2$ : 0.59 ppm) flowing in a levitation furnace. Fig. 1 shows a macrostructure of the cross section of the melted ingot. The alloyed part was chemically analyzed at the 10 cross points of the black lines. Chemical composition was very homogeneous except at the LS point, which is close to the fusion line between the melted part and the un-melted skull. No difference of composition was detected between the equiaxed and cylindrical crystal zones. The composition except the skull part was V- (4.50- 4.57)Cr- (4.56- 4.78)Ti- (0.09- 0.10)Y- (0.009- 0.013)C- (0.012- 0.015)N- (0.008- 0.013)O. Fig. 2 shows X-ray diffraction spectrum at the place pointed by arrows indicated in Fig. 1.  $Y_2O_3$  compound was clearly detected at the top and side skin of the ingot. A weak peak from  $Y_2O_3$  (circled) also detected at the inner surface of the void. The ingot was trimmed to remove the skin, the void containing  $Y_2O_3$  slug, and the un-alloyed skull, followed by cold rolling into sheets with 0.25-4 mm in thickness.

Fig. 3 shows hardness recovery by annealing (873-1373 K for 1 hr) and precipitation treatment (1373 K for 1 hr + 973 K for 1 hr) in the 1 mm-thick sheet. From 1073 K to 1273 K annealing, hardness of the Y-added alloy was similar to NIFS-HEAT (NH1). At 1373 K annealing, NH1 has shown hardening compared with 1273 K, whereas the Y-added alloy indicated no hardening. In the precipitation treatment, NH1 exhibited significant hardening. In contrast, the hardening in Y-added alloy was much smaller. The precipitates contributing the hardening were identified as Ti-O type by microstructural observations. Their size and number density was 20 nm and  $7.3 \times 10^{19} m^{-3}$  for NH1, while 35 nm and  $3.3 \times 10^{18} m^{-3}$  for the Y-added alloy. The small number density is considered to result in the smaller hardening in the Y-added alloy. As  $Y_2O_3$  precipitates were also detected in the Y-added alloy, O was thought to be stabilized as  $Y_2O_3$ , which can reduce oxygen amount in the Ti-O type precipitates and in solid solution state. Since O in solution interacts with irradiation defects, neutron irradiation hardening and embrittlement is expected to be improved by the Y addition.

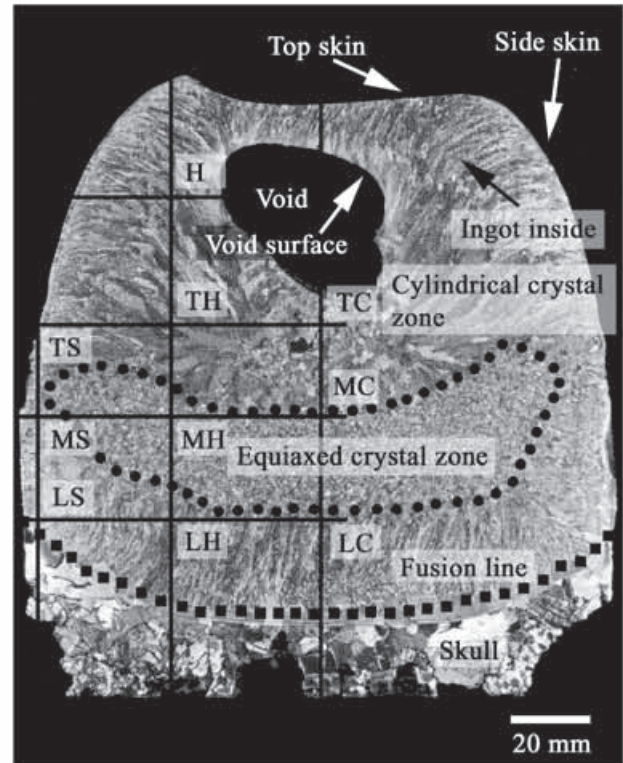


Fig. 1 Cross section of a V-4Cr-4Ti-0.15Y ingot fabricated by levitation melting.

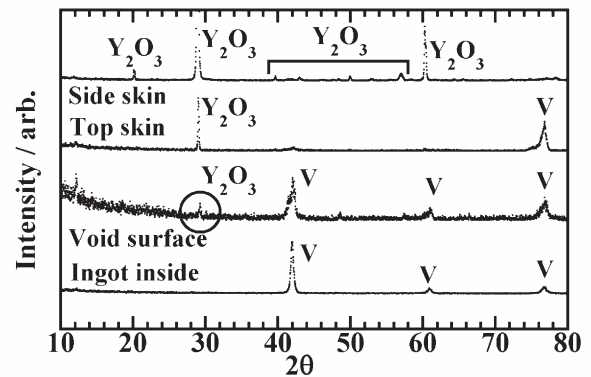


Fig. 2 XRD spectrum at the place pointed by arrows in Fig. 1.

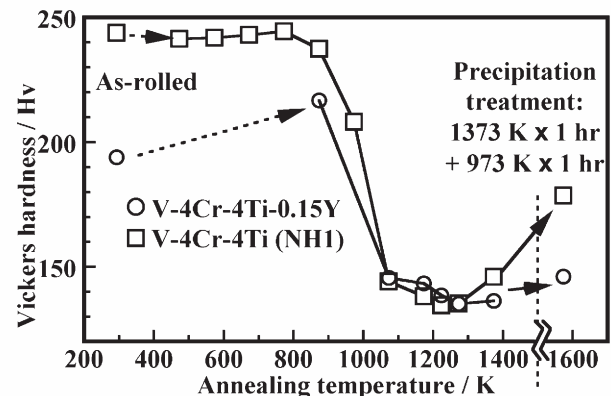


Fig. 3 Recovery of hardness by annealing (873-1373 K) and precipitation treatment (1373 K then 973 K) in the cold-rolled sheet.